J Membrane Biol (2013) 246:391–397
DOI 10.1007/s00232-013-9545-8

Bisphenol A Modulates Calcium Currents and Intracellular Calcium Concentration in Rat Dorsal Root Ganglion Neurons

Wenjuan Wang · Jun Wang · Qiang Wang · Wenhui Wu · Fei Huan · Hang Xiao

Received: 6 December 2012 / Accepted: 29 March 2013 / Published online: 11 April 2013

Abstract The endocrine-disrupting chemical bisphenol A (BPA) is used to manufacture plastics including food containers, and it may leach into these containers. Consumption of BPA that has leached out of plastics may be harmful as recent research highlighted that BPA can induce alterations in the nervous system. In the present work, we studied the effects of BPA on Ca^{2+} channels in dorsal root ganglion (DRG) neurons. Using whole-cell patch-clamp recordings, we found that I_{Ca} could be reduced by BPA in a concentration-dependent manner. Additionally, BPA shifted the activation curve of calcium currents toward a depolarizing direction and increased the slope factor of the curve. The inactivation curve for the currents was also assessed, and the curve shifted toward the depolarizing direction, although it was not significant. Moreover, inhibitory effects of BPA on the increments of intracellular Ca^{2+} concentrations ($[Ca^{2+}]_i$) induced by 50 mM KCl were observed in DRG neurons using a laser scanning confocal microscopy assay. Further work revealed that the PKA and PKC pathways may be involved in the inhibitory effects of BPA since the PKA antagonist GÖ-6983 and the PKC antagonist H-89 significantly alleviated the inhibitory effects of BPA on I_{Ca}. As such, the results of the present study provide direct evidence that BPA decreases I_{Ca} and impairs calcium homeostasis, which may be involved in any toxic effects of BPA on DRG neurons.

Keywords Bisphenol A · Ca^{2+} channel · Protein kinase C · Protein kinase A · Dorsal root ganglion neuron

Introduction

Bisphenol-A (2,2-bis[4-hydroxyphenyl[-propane [BPA]) has been found to be an endocrine disruptor and is widely used in the manufacture of polycarbonate and epoxy resins. The major source of human exposure to BPA is from food containers (e.g., milk, water and infant bottles) and medical devices (Suzuki et al. 2000). Humans are primarily exposed to BPA when they consume water and milk from containers or packages that were manufactured using this chemical (Vandenberg et al. 2007) because BPA can leach into the milk or water from these containers or packages. BPA has been detected in multiple tissue compartments including urine, saliva, breast milk and adipose tissue (Dong et al. 2011). Previous studies have demonstrated that BPA may have adverse effects on reproductive function (Savabieasfahani et al. 2006), metabolism (Hugo et al. 2008) and the immune system (Sawai et al. 2003). It is worth mentioning that BPA is able to directly influence neuronal functions as well. For example, BPA modifies the activity of neural pathways involved in nociception and pain (Aloisi et al. 2002) and inhibits estradiol-induced hippocampal synaptogenesis (MacLusky et al. 2005).

The α and β estrogen receptors (ERα and ERβ) can activate genomic signals and have been reported to be the foremost molecular mediators of the in vitro and in vivo

W. Wang
School of Public Health, Guiyang Medical University, 9 Beijing Road, Guiyang 550004, China

W. Wang · J. Wang · W. Wu · F. Huan · H. Xiao (✉)
Department of Toxicology, School of Public Health, 140 Hanzhong Road, Nanjing, Jiangsu 210029, China
e-mail: reality0337@163.com; hxiao@njmu.edu.cn

Q. Wang
Department of Preventive Medicine, School of Medical Science and Laboratory Medicine, Jiangsu University, 301 Xuefu Road, Zhenjiang 212013, China

effects exerted by BPA (Hall and Korach 2002). Besides genomic activation, accumulating data show that BPA affects ion channel function via nongenomic estrogenic actions and subsequently alters rapid signals. Our recent results also revealed that BPA could rapidly inhibit I_{Na}, which might result from the rapid activation of Na^+ channels (Wang et al. 2011).

Voltage-gated Ca^{2+} channels mediate intracellular Ca^{2+} homeostasis in response to modulation in membrane potentials, thereby contributing to some neuronal reactions such as nociceptive transmission. Furthermore, the phosphorylation of PKA and PKC is a key component of the calcium-handling machinery including Ca^{2+}-ATPase of estrogen receptor membranes and calcium channels (Yang et al. 2004). With these data in mind, we hypothesized that the calcium channels, accompanied by the downstream signaling pathways PKA and PKC, might be involved in BPA-regulated Ca^{2+} homeostasis.

Materials and Methods

All experiments were conducted in accordance with the NIH "Guide for the Care and Use of Laboratory Animals," and the study was approved by the local institutional animal care and use committee.

Isolation of Dorsal Root Ganglion Neurons

Male Sprague–Dawley rats (5–6 weeks old) were anesthetized with ether and then rapidly decapitated. The thoracic and lumbar segments of the spinal cord were dissected. The ganglion fragments were placed in a flask containing 5 ml of Hank's Balanced Salt Solution (HBSS), type I collagenase (3 mg) and type I trypsin (1 mg) at 36.5 °C for 35 min. Single neuron bodies were obtained by trituration in standard external solution, plated onto a 35-mm culture dish and incubated for at least 1 h before electrophysiological recordings were conducted. Freshly isolated neurons from the rat dorsal root ganglion (DRG) in the range of 20–40 mm (small- to medium-sized) were used in the present study.

Solutions and Chemicals

The ionic composition of HBSS consisted of (in mM) 130 NaCl, 5 KCl, 0.3 KH_2PO_4, 4 $NaHCO_3$, 0.3 Na_2HPO_4 and 10 glucose; the pH was about 7.3–7.4, adjusted with NaOH. The standard external solution was (in mM) 130 NaCl, 5 KCl, 5 $CaCl_2$, 2 $MgCl_2$, 10 HEPES and 10 D-glucose; the pH was adjusted to 7.3 with NaOH.

For voltage-clamp experiments, the internal solution consisted of (in mM) 125 CsCl, 2 $MgCl_2$, 20 HEPES, 11 EGTA, 1 $CaCl_2$, 4.5 Mg-ATP and 0.3 Li-GTP; the pH was adjusted to 7.3 with CsOH. The extracellular solution for recording of I_{Ca} contained (in mM) 140 tetraethylammonium-Cl (TEA-Cl), 5 $CaCl_2$, 0.8 $MgCl_2$, 10 HEPES and 11 D-glucose; the pH was 7.3, adjusted with Tris-base.

BPA, collagenase (type I), trypsin (type I), H-89, GÖ-6983, dimethylsulfoxide (<0.1 %), HEPES, KCl, CsCl, $CdCl_2$, EGTA, TEA-Cl, Mg-ATP, Li-GTP, Fluo-3/AM, nifedipine, ω-comtoxin MVIIC and ω-comotoxin MVIIA were all purchased from Sigma (St. Louis, MO). All other chemical reagents used were of analytic grade.

Electrophysiological Recordings

Neurons were recorded in the whole-cell patch configuration using an EPC-9 amplifier and Pulse 8.02 software (HEKA Elektronik, Pfalz, Germany). After establishing the whole-cell mode, capacitive transients were canceled with the amplifier. Series resistance was compensated between 60 and 80 %.

Calcium Imaging

Isolated DRG neurons were suspended in the standard external solution, incubated with 5 μl Fluo-3/AM at 37 °C for 30 min, washed and imaged in the standard external solution. Dishes were mounted in an experimental chamber and placed on an inverted microscope that connected to a laser scanning imaging system (LSM510; Zeiss, Oberkochen, Germany). High-KCl isotonic solutions were prepared by decreasing the concentration of NaCl to 85 mm and leaving the other components of the solution unchanged. Fluo-3/AM was excited at 488 nm with an argon ion laser, and its emitted fluorescence was measured at 520 nm.

Data Analysis

All statistical comparisons were conducted using Student's t test, and statistical significance was accepted at $P < 0.05$. The concentration-dependent inhibitory effects were fitted with the Hill equation: $I/I_{max} = 1 - [BPA]^H/IC_{50}^H + [BPA]^H$, where I/I_{max} are the observed and maximum blocking percentages of current, BPA is the concentration of the drug, IC_{50} is the concentration producing a half-maximal current block and H is the Hill coefficient. The voltage dependence of I_{Ca} activation was fitted with the Boltzmann equation: $G/G_{max} = 1/(1 + \exp(((V_{g0.5} - V_m)/k_g)))$, where G_{max} is the maximal potential conductance and $V_{g0.5}$ and k_g are the potential at which G/G_{max} reaches its half-maximal value and the slope factor, respectively. The curve of voltage dependence of the steady-state I_{Ca} inactivation

was fitted according to the Boltzmann equation: $I/I_{max} = 1/(1 + \exp((V_h - V_{h0.5})/k_h))$, where I_{max} is the maximum of peak currents, V_h is the prepulse potential and $V_{h0.5}$ and k_h are the voltage for half-inactivation potential and the slope factor, respectively. In all cases, the fluorescence intensity was normalized to its initial value recorded in normal DRG cells before KCl application ($F0$) and is expressed as the relative amplitude fluorescence $(F - F0)/F$.

Results

Concentration-Dependent Effects of BPA on I_{Ca}

To explore the effects of BPA on Ca^{2+} channels in DRG neurons, the whole-cell patch-clamp technique was performed. Inward currents were elicited by 0 mV, 80-ms depolarizing pulses with a holding potential of −90 mV; they were completely blocked by perfusion of 100 μM $CdCl_2$ and then defined as I_{Ca} (Fig. 1a).

Significant declines in I_{Ca} were observed after treatment with BPA for 5 min, and these currents were partly reversed after 3-min washout (Fig. 1b). To identify the specific effects of BPA on Ca^{2+} channels, varied doses of BPA (0.1, 1, 10, 50 and 100 μM) were used. Peak currents were measured before and after 5 min of treatment with BPA, and the data were collected from eight different cells for each concentration of BPA. The mean inhibition values of the peak current fraction were fitted with the Hill equation. The fitting curve revealed an $IC_{50} = 11.60$ μM (Fig. 1c).

Effects of BPA on I_{Ca} Amplitude and Kinetics

To investigate the effects of BPA on the I–V curve of I_{Ca} in DRG neurons, cells were stimulated with depolarizing pulses between −60 and 40 mV in 10-mV increments with membrane potential held constant at −90 mV (Fig. 2a). The I_{Ca} was activated at about −35 mV, and the peak amplitude occurred at about 0 mV (Fig. 2b), in line with the known characteristics of high voltage–activated (HVA) I_{Ca} (Carbone et al. 1997). After 5-min application of 10 μM BPA, the current density at the peak amplitude decreased from −80.16 ± 18.30 to −45.69 ± 20.92 pA/pF ($n = 6$, $P < 0.05$) and the peak current potential shifted from 0 to −10 mV.

The same protocol was used to study the dynamic properties of Ca^{2+} channels. The activation curve of I_{Ca} was fitted with a Boltzmann function. As shown in Fig. 2c, $V_{g0.5}$ shifted in the depolarizing direction from −20.13 ± 0.59 to −9.78 ± 3.93 mV after treatment with 10 μM BPA ($n = 6$, $P < 0.05$). K_g increased from 4.29 ± 0.59 to 8.25 ± 2.03 after BPA perfusion ($n = 6$, $P < 0.05$).

Steady-state inactivation was examined using a two-pulse protocol. It consisted of a series of prepulses (from −90 to 30 mV in 10-mV increments) lasting 500 ms from a holding potential of −90 mV, followed immediately by a

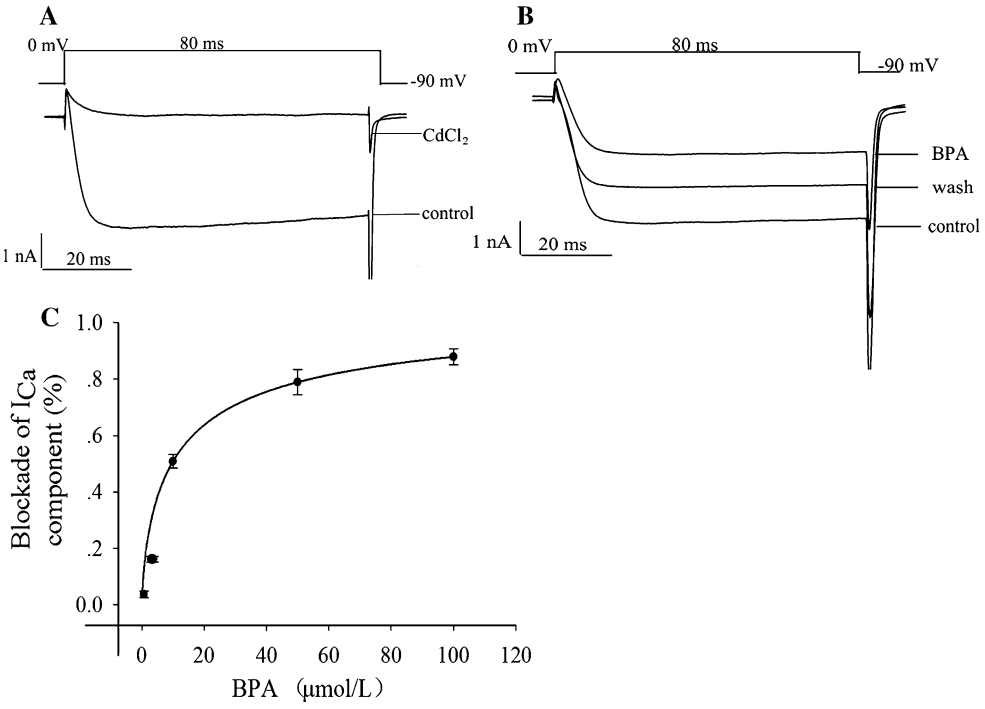

Fig. 1 Inhibition of I_{Ca} by BPA in rat DRG neurons. **a** Currents were elicited by depolarizing steps of 80-ms duration to 0 mV from a holding potential of −90 mV. These currents were blocked by 100 μM $CdCl_2$. **b** Typical I_{Ca} trace before and after 5-min treatment with BPA (10 μM). **c** Concentration–response data for BPA in I_{Ca} inhibition. Note that the IC_{50} value is 11.60 μM ($n = 8$)

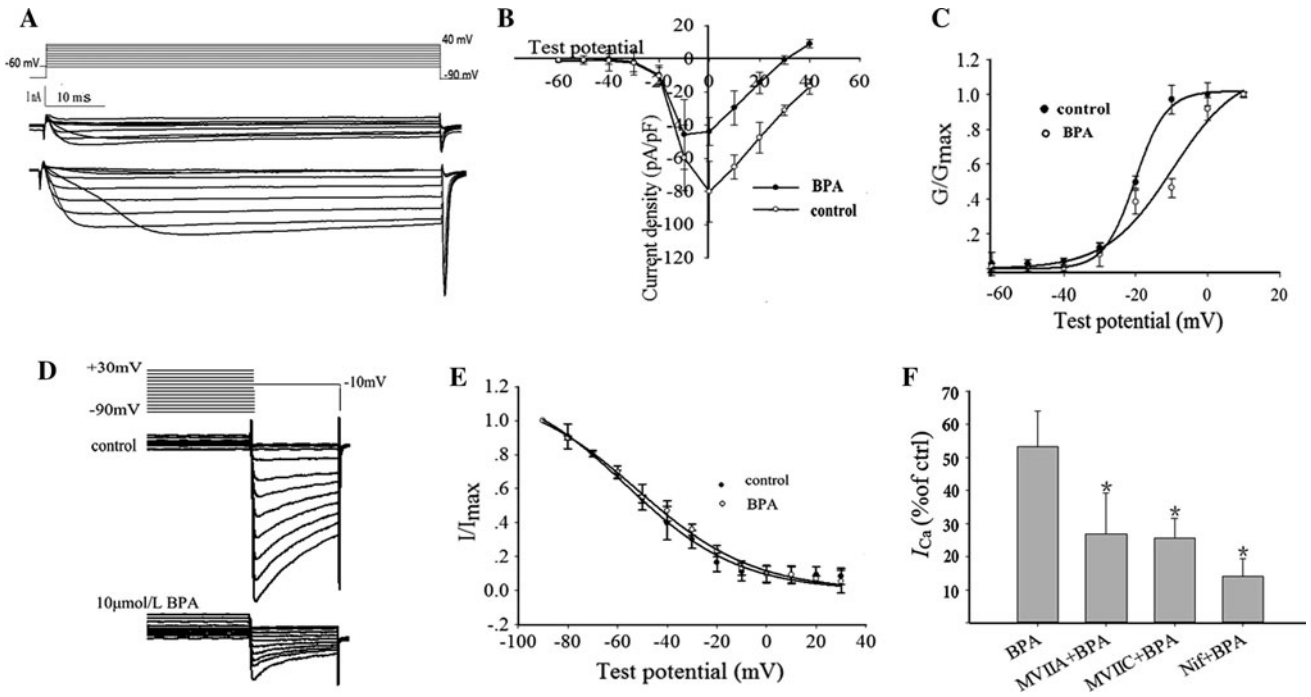

Fig. 2 Effects of BPA on I_{Ca} amplitude and kinetics. **a**, **d** Activation and inactivation of Ca^{2+} current families before and after BPA (10 μM) perfusion. **b** Current–voltage (*I–V*) relationship of I_{Ca} in the control and BPA (10 μM) treatment groups ($P < 0.05$, $n = 7$). **c** Activation curves were drawn after fitting with a Boltzmann function ($n = 6, P < 0.05$). **e** Currents normalized with maximal control current were plotted against the prepulse potentials. Inactivation curves were drawn after fitting with a Boltzmann function ($n = 6$, $P > 0.05$). **f** Effects of BPA on the HVA subtypes of currents (mean ± SEM, $n = 6$). After treatment with nifedipine, ω-comtoxin MVIIC and ω-comotoxin MVIIA, the decrease in I_{Ca} induced by BPA (10 μM) was 14.02 ± 2.51 %, 25.66 ± 3.99 % and 26.90 ± 5.33 %, respectively. *Significant ($P < 0.05$) decrease compared to BPA values

depolarizing pulse to −10 mV (Fig. 2d). The steady-state inactivation parameter was fitted using the Boltzmann equation (Fig. 2e). However, BPA did not significantly affect the inactivation curve (control, $V_{h0.5} = -56.26 \pm 4.42$ mV, $K_h = -22.68 \pm 2.05$; BPA, $V_{h0.5} = -51.92 \pm 2.85$ mV, $K_h = -23.41 \pm 1.39$; $n = 6, P > 0.05$).

Effects of BPA on the Voltage-Gated Ca^{2+} Channel Subtypes of Currents

To determine whether BPA differentially affects the subtypes of HVA I_{Ca}, we isolated L-, P/Q- and N-type channel currents and tested them separately for their sensitivity to BPA. Preincubation of the selective L-type Ca^{2+} channel antagonist nifedipine (at 10 μM) decreased the inhibitory effects of BPA (10 μM, 14.02 ± 5.51 %). Similarly, preincubation with the P/Q-type Ca^{2+} channel antagonist ω-comtoxin MVIIC (at 2 μM) decreased the inhibitory effects of BPA on I_{Ca} to 25.66 ± 5.99 %. Moreover, preincubation with the selectively N-type Ca^{2+} channel antagonist ω-comotoxin MVIIA (2 μM) decreased the inhibitory effects BPA on I_{Ca} to 26.90 ± 12.33 % (Fig. 2f).

PKA and PKC Were Involved in BPA-Induced Inhibitory Effects

The protein kinases PKA and PKC, which are intimately involved in Ca^{2+} homeostasis, may modulate the function of Ca^{2+} channels (Ramirez-Correa et al. 2010). Therefore, we next investigated whether the downstream intracellular signaling pathways PKA and PKC participated in the inhibitory effects of BPA (10 μM) on I_{Ca}. In this regard, preincubation of rat DRG neurons with the PKA inhibitor H-89 (2 μM) significantly decreased the inhibitory effects of BPA on I_{Ca} (inhibition rate = 22.3 ± 3.70 %, $n = 6$, Fig. 3a). Similarly, pretreatment with the PKC inhibitor GÖ-6983 (1 μM) partially eliminated the BPA-mediated inhibitory effects of I_{Ca} (inhibition rate = 18.80 ± 3.91 %, $n = 6$, Fig. 3b). In addition, H-89 (2 μM) and GÖ-6983 (1 μM) did not affect basal I_{Ca} notably.

BPA Inhibited KCl-Invoked Calcium Transients

With confocal microscopy, we found that fast perfusion for approximately 10 s of 50 mM KCl caused transient increases

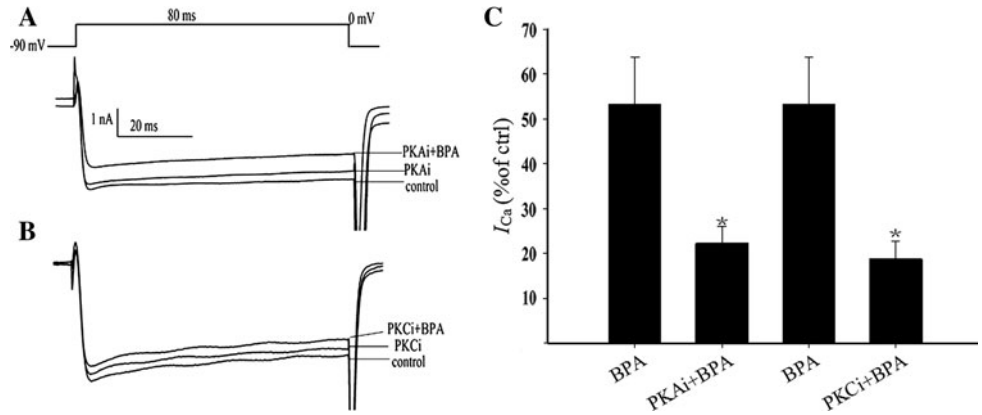

Fig. 3 Effects of BPA in the presence of PKC and PKA inhibitors. I_{Ca} amplitude was obtained via depolarizing steps to 0 mV from a holding potential of −90 mV. **a** H-89 (2 μM), a PKA inhibitor, had no effect on I_{Ca} and prevented BPA-induced inhibition. **b** Likewise, GÖ-6983 (1 μM), a PKC inhibitor, had no effect on the I_{Ca} but prevented the ability of BPA to decrease the current. **c** The influence of GÖ-6983 and H-89 on the inhibitory effects of BPA on I_{Ca} in DRG neurons. *Significant ($n = 6$, $P < 0.05$) decrease compared to BPA values

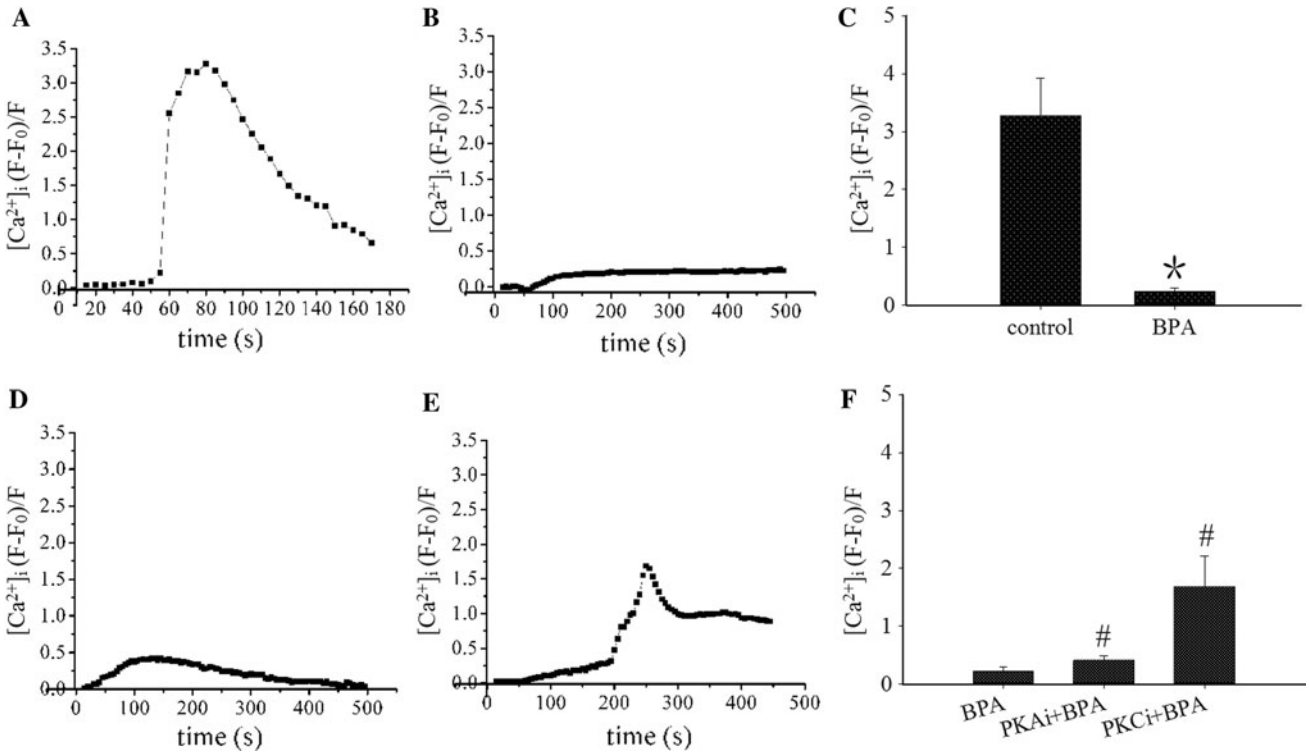

Fig. 4 Ca^{2+} signaling induced by KCl in DRG neurons. **a** Selected images taken at different times during the exposure to 50 mM KCl showing a representative neuron responding with transient increases in $[Ca^{2+}]_i$ over a basal level. **b** Representative experiment showing that pretreatment with BPA (10 μM, 20 min) decreased the peak of the KCl-induced $[Ca^{2+}]_i$ transient. **c** Group data showing that the calcium elevation induced by KCl in DRG neurons was markedly attenuated in the presence of BPA. *Significant ($P < 0.05$) decrease compared to the control groups. **d**, **e** Representative tracings showing the effects of BPA (10 μM) on Ca^{2+} oscillations in the neurons treated with H-89 (5 μM) and GÖ-6983 (5 μM). **f** Summary data of preincubation with H-89 (5 μM) and GÖ-6983 (5 μM) on the attenuation action of BPA. All experiments were repeated three times using different batches of cells. $^{\#}P < 0.05$ compared to BPA (10 μM) treatment groups

in $[Ca^{2+}]_i$ (327.91 ± 64.30 %), which returned to the basal level within 180 s (Fig. 4a). However, treatment with BPA (10 μM) markedly inhibited the increment of $[Ca^{2+}]_i$ evoked by 50 mM KCl ($P < 0.05$) with peak amplitudes decreased to 23.06 ± 6.40 % ($n = 5$, $P < 0.05$), and the $[Ca^{2+}]_i$ did not return to basal levels within 500 s (Fig. 4b).

To explore whether PKA and PKC were associated with the inhibitory effects of BPA on KCl-evoked $[Ca^{2+}]_i$ transients, the PKA and PKC blockers were applied. As shown in Fig. 4d, pretreatment with H-89 (5 μM, 20 min) prevented the inhibitory effects of BPA (10 μM) (from 23.06 ± 5.40 to 41.18 ± 8.10 %; $n = 8$, $P < 0.05$) on KCl-evoked Ca^{2+} transients in DRG neurons. Similar results were also observed following pretreatments with GÖ-6983 (5 μM, 20 min; Fig. 4e; 168.71 ± 52.10 %; $n = 7$, $P < 0.05$). Taken together, these results indicate that the PKA and PKC signaling pathways may participate in the inhibitory effects of BPA on Ca^{2+} transients.

Discussion

In the present study, we investigated, for the first time, the effects of BPA on Ca^{2+} channels in DRG neurons. The results revealed that BPA suppressed I_{Ca} in rat DRG neurons in a concentration-dependent manner, with an IC_{50} of 11.60 μM. Further results revealed that the activation curve shifted to the depolarizing direction after exposure to BPA, while no obvious shifting of the inactivation curve was observed. These results implied that BPA could interact with the active state of the Ca^{2+} channels and reduce the frequency of Ca^{2+} channel opening following voltage stimulation, which is responsible for the reductions in peak I_{Ca}. In addition, the *I–V* curves of the total I_{Ca} in our experiments showed that the threshold for activation is −35 mV and the maximal peak current occurs at 10 or 0 mV, in line with the known characteristics of HVA Ca^{2+} channels (Carbone et al. 1997).

As previously described, DRG neurons were classified into three groups: small-sized, medium-sized and large-sized neurons (Greffrath et al. 2009). The vast majority of DRG neurons, particularly the small- and medium-sized cells, are nociceptive; and their peripheral terminals are specialized to detect actual or potential tissue damage (Greffrath et al. 2009). Based on the idea that BPA alters the ion channel switch selectivity of calcium currents and to highlight the effects of BPA on the different channel subtypes, subsets of experiments were performed. Our examinations of L-, N- and P/Q- type calcium channel currents before and after the application of BPA illustrated that all three subtypes were partially inhibited by BPA. As reported, L-type Ca^{2+} channels may make a major contribution to the transient rise in $[Ca^{2+}]_i$ when unclamped DRG neurons are activated by external stimulation (Greffrath et al. 2001). The present study shows that the inhibitory effects of BPA in large part depend on L-type voltage-gated Ca^{2+} channel currents, which make important contributions to decrease the excitability of primary afferent neurons.

The capacity of neurons to respond to membrane depolarization with a Ca^{2+} signal is an essential function, which can be used as a parameter to study the development and maturation of neurons in cultures. In the present work, we found that BPA markedly inhibited $[Ca^{2+}]_i$ invoked by KCl, which is similar to the stimulation of the depolarization pulse performed by the patch-clamp amplifier (Sharma et al. 2010). It is worth mentioning that the $[Ca^{2+}]_i$ induced by KCl did not return to basal levels within 500 s, which may due to the mobilization of BPA on intracellular Ca^{2+} via the endoplasmic reticulum (Tanabe et al. 2006).

Previous reports have shown that protein kinases, such as PKA and PKC, may modulate the function of Ca^{2+} channels (Kamp and Hell 2000; Keef et al. 2001). Additionally, to analyze a potential involvement of PKC in the modulation of $I_{Ca(V)}$ by myricetin, PKC was inhibited by preincubation with chelerythrine 30 min before application of myricetin (Hagenacker et al. 2010). However, application of the inhibitor alone did not affect $I_{Ca(V)}$. Our results were consistent with these reports that pretreatment with H-89 and GÖ-6983 (which did not alter basal Ca^{2+} currents, as shown in Fig. 4) partially eliminated the BPA-induced inhibitory effects on I_{Ca} as well as the KCl-evoked increments of $[Ca^{2+}]_i$, suggesting that both the PKA and PKC pathways are involved in the BPA-mediated inhibitory effects on Ca^{2+} channels. These results are in line with previous studies showing that BPA is closely involved in PKC and PKA activation (Bouskine et al. 2009).

In conclusion, in this study, we investigated the inhibitory effects of BPA on voltage-gated calcium channels and $[Ca^{2+}]_i$ transients invoked by KCl in DRG neurons via a nongenomic process that involved both the PKC and PKA signaling pathways. In conjunction with previous studies, these results suggest that BPA has cytotoxic effects in the nervous system and provide new insight into the mechanisms underlying this toxicity. Further studies should elucidate the cellular signaling mechanisms that mediate BPA-induced elevations of $[Ca^{2+}]_i$ invoked by KCl as this will further enhance our understanding of the physiological effects of BPA.

Acknowledgments This work was supported by the National Natural Science Foundation of China (Grant 81072329); the Innovation Project of Graduate Education of the Higher Education Institutions of Jiangsu Province, China (grant CX10B_348Z); and a project funded by the Priority Academic Program Development of Jiangsu Higher Education Institutions.

References

Aloisi AM et al (2002) Exposure to the estrogenic pollutant bisphenol A affects pain behavior induced by subcutaneous formalin injection in male and female rats. Brain Res 937(1–2):1–7

Bouskine A et al (2009) Low doses of bisphenol A promote human seminoma cell proliferation by activating PKA and PKG via a membrane G-protein-coupled estrogen receptor. Environ Health Perspect 117(7):1053–1058

Carbone E et al (1997) Ca^{2+} and Na^{+} permeability of high-threshold Ca^{2+} channels and their voltage-dependent block by Mg^{2+} ions in chick sensory neurones. J Physiol 504(Pt 1):1–15

Dong S, Terasaka S, Kiyama R (2011) Bisphenol A induces a rapid activation of Erk1/2 through GPR30 in human breast cancer cells. Environ Pollut 159(1):212–218

Greffrath W et al (2001) Changes in cytosolic calcium in response to noxious heat and their relationship to vanilloid receptors in rat dorsal root ganglion neurons. Neuroscience 104(2):539–550

Greffrath W et al (2009) Heat-induced action potential discharges in nociceptive primary sensory neurons of rats. J Neurophysiol 102(1):424–436

Hagenacker T et al (2010) Anti-allodynic effect of the flavonoid myricetin in a rat model of neuropathic pain: involvement of p38 and protein kinase C mediated modulation of Ca^{2+} channels. Eur J Pain 14(10):992–998

Hall JM, Korach KS (2002) Analysis of the molecular mechanisms of human estrogen receptors alpha and beta reveals differential specificity in target promoter regulation by xenoestrogens. J Biol Chem 277(46):44455–44461

Hugo ER et al (2008) Bisphenol A at environmentally relevant doses inhibits adiponectin release from human adipose tissue explants and adipocytes. Environ Health Perspect 116(12):1642–1647

Kamp TJ, Hell JW (2000) Regulation of cardiac L-type calcium channels by protein kinase A and protein kinase C. Circ Res 87(12):1095–1102

Keef KD, Hume JR, Zhong J (2001) Regulation of cardiac and smooth muscle Ca^{2+} channels (CaV1.2a, b) by protein kinases. Am J Physiol Cell Physiol 281(6):C1743–C1756

MacLusky NJ, Hajszan T, Leranth C (2005) The environmental estrogen bisphenol A inhibits estradiol-induced hippocampal synaptogenesis. Environ Health Perspect 113(6):675–679

Ramirez-Correa GA et al (2010) Calcium sensitivity, force frequency relationship and cardiac troponin I: critical role of PKA and PKC phosphorylation sites. J Mol Cell Cardiol 48(5):943–953

Savabieasfahani M et al (2006) Developmental programming: differential effects of prenatal exposure to bisphenol-A or methoxychlor on reproductive function. Endocrinology 147(12):5956–5966

Sawai C, Anderson K, Walser-Kuntz D (2003) Effect of bisphenol A on murine immune function: modulation of interferon-gamma, IgG2a, and disease symptoms in NZB $\times$ NZW F1 mice. Environ Health Perspect 111(16):1883–1887

Sharma R et al (2010) Effects of ethanol on extracellular levels of adenosine in the basal forebrain: an in vivo microdialysis study in freely behaving rats. Alcohol Clin Exp Res 34(5):813–818

Suzuki K et al (2000) Content and release of bisphenol A from polycarbonate dental products. Dent Mater J 19(4):389–395

Tanabe N, Kimoto T, Kawato S (2006) Rapid Ca^{2+} signaling induced by bisphenol A in cultured rat hippocampal neurons. Neuro Endocrinol Lett 27(1–2):97–104

Vandenberg LN et al (2007) Human exposure to bisphenol A (BPA). Reprod Toxicol 24(2):139–177

Wang Q et al (2011) Inhibition of voltage-gated sodium channels by bisphenol A in mouse dorsal root ganglion neurons. Brain Res 1378:1–8

Yang HW et al (2004) Roles of CaMKII, PKA, and PKC in the induction and maintenance of LTP of C-fiber-evoked field potentials in rat spinal dorsal horn. J Neurophysiol 91(3):1122–1133